This is a post-peer-review, pre-copyedit version of an article published in *Applied Surface Science*. The final authenticated version is available online at: https://doi.org/10.1016/j.apsusc.2021.150911

# Functionalization of synthetic saponite: identification of grafting sites and application for anions sequestration

Gustave Kenne Dedzo[1], Severinne Rigolet[2], Ludovic Josien[2], Emmanuel Ngameni[1], and Liva Dzene[2]*

[1]Laboratory of Analytical Chemistry, Faculty of Science, University of Yaoundé I, B.P. 812, Yaoundé, Cameroon

[2]Institut de Science des Matériaux de Mulhouse CNRS UMR 7361, Université de Haute-Alsace, Université de Strasbourg, 3b rue Alfred Werner, 68093 Mulhouse, Cedex, France

E-mail: liva.dzene@uha.fr

Tel.: + 33 3 89 33 67 38

## Abstract

The present work reports the study of the mechanism of grafting of an alkoxysilane on the surface of a synthetic saponite. XRD and SEM/EDX characterizations confirmed the effective synthesis of the clay mineral with structural formula $^{INT}Na_{0.50}{}^{TET}[Si_{3.50}Al_{0.50}]^{OCT}[Mg_3]O_{10}(OH)_2$. The functionalization of this material in its pristine or acid pre-treated form with a cationic silane (tetradecyldimethyl(3-trimethoxysilylpropyl)ammonium chloride) yielded a nanohybrid organoclay with interesting structural and chemical properties highlighted by $^{29}Si$ solid state NMR, XRD, FTIR, TGA and electrochemical characterizations. The monodentate and bidentate grafting of the alkoxysilane was observed regardless the starting material was pristine or acid pre-treated saponite. The more significant layer-to-layer distance increase observed after the functionalization of acid pre-treated saponite indicated some interlayer intercalation/grafting of the alkoxysilane. Electrochemical characterization (cyclic voltammetry and electrochemical impedance

spectroscopy) showed that the modified clay mineral exhibited anionic exchange property due to the presence of grafted cationic alkoxysilane. This anionic exchange capacity was confirmed when successfully applied for the adsorption of the anionic dye Congo Red. In all cases, the acid pre-treatment tended to improve the anion exchange property of the organoclay.

Keywords: Synthetic saponite, Alkoxysilane, Grafting, Anionic exchange capacity, Electrochemical characterization

# 1. Introduction

The quantity of generated wastewater increases globally due to the growth of human population and growing industrial activity in developing countries. Yet, accordingly to United Nations, 80% of wastewater is returned in ecosystem without any treatment mainly in low-income areas in developing countries [1]. Therefore, there is always a quest for cheap and local adsorbents capable to treat wastewater. Clay minerals enlist among most abundant adsorbent materials, and are very often the first choice for local wastewater treatment [2]. Indeed, they have excellent ion-exchange properties. However, pristine clay minerals are able to adsorb only positively charged species, inorganic and organic cations. Therefore, the functionalization is needed to increase the range of possible species to be adsorbed, i.e. neutral and negative species.

The functionalization of the surface of silica and other aluminosilicate particles can be achieved by silylation (grafting of trialkoxysilanes) [3]. The incredible variety of the functional group of the trialkoxysilanes allows tuning the surface chemical properties of materials. The formation of covalent bond through hydrolysis and condensation reactions between the surface of the solid particles and alkoxysilane compound during the silylation, stabilizes the organic component and prevents its leaching during application. Among different porous materials, clay minerals were reported to have the highest amount of alkoxysilane grafted per unit of surface area [4]. Clay minerals are layered aluminosilicates. As such, the clay mineral particles have different types of surfaces: interlayer and external (basal and edge) surfaces. Takahashi&Kuroda [5] reviewed the modification of different layered silicates by silylation focusing solely on the interlayer surfaces. In practice, the functionalization of interlayer surfaces by covalent grafting of alkoxysilanes has proved to be challenging. There are various factors influencing the silylation rate, e.g. crystal defects [6] and solvent type [7]. It has been noted previously that among other factors, the silylation rate would depend also on the reactivity of clay mineral surfaces [8,9]. For swelling clays (smectites), it is actually the edge surface which is expected to have higher reactivity due to the presence of ≡O-H groups. Different possibilities of grafting reactions occurring on clay mineral surfaces have been suggested [10–12]. The proposed mechanisms distinguish 4 cases: (1) monodentate grafting on the edge surface without modification of layer-to-layer distance, (2) bidentate grafting on the edges with the increase of layer-to layer distance, (3) grafting and/or intercalation with partial condensation in the interlayer surface with increase of layer-

to-layer distance, (4) random grafting on all surfaces with loss of periodicity of layer-to-layer stacking. Previous studies of smectite silylation had reported all four mechanisms. In case of hectorite, a magnesian swelling clay mineral, the grafting of alkoxysilanes had been reported occurring mainly on the edge surface of particles without a significant change of layer-to-layer distance within particles [12–14]. For montmorillonite, an aluminian swelling clay, the grafting had been reported occurring mainly in the interlayer surface [7,15–17], edge surfaces [18] or randomly on different surfaces [10,19–21]. Similarly, the grafting on different surfaces had been suggested for the saponite [11,22], magnesian swelling clay mineral similar to hectorite. Thus, systematic knowledge about the influence of different parameters on the grafting mechanism and involved surfaces is lacking. In consequence, the lack of a detailed knowledge of functionalization mechanism leads to the waste of chemicals during the preparation process of the materials.

For a detailed understanding of such mechanisms, the use of natural clay minerals is challenging. Natural samples are very often heterogeneous, since they contain different mineral phases. The presence of trace elements and structural defects render difficult the interpretation of experimental results. To overcome this challenge, synthetic clay minerals can be used. Moreover, the use of synthetic clay minerals can make it possible to obtain materials with well-controlled properties. The methods of synthesis of the different types of clay minerals have been periodically reviewed [23–25]. The synthesis of saponite, swelling magnesian smectite, is relatively easy, allowing to obtain samples with controlled chemistry and particle size [24,26–28]. Moreover, only few studies report the silylation of saponite and especially the application of such materials.

Thus, in this work we aim to synthesize saponite clay mineral and to study the possible sites of functionalization by a cationic trialkoxysilane. Since the reactivity of edge surface is expected to be the highest, the hypothesis explored is that the alkoxysilane reacts primarily with edge surfaces of saponite. The strategy consists of functionalizing first an unmodified saponite sample to probe the sites located on the edge and basal surfaces of particles. An acid pre-treatment is then subsequently applied aiming to functionalize the interlayer surface as in the case with other smectites [29,30]. The physicochemical and electrochemical characterizations are then performed to highlight the subtle modifications of the chemical properties of the materials following its surface functionalization. The trialkoxysilane used being cationic, the overall charge of the modified saponite is then expected to decrease

(becoming less negative or cationic for a high degree of functionalization). Such materials can be exploited for the sequestration or removal of anionic compounds. In this work, Congo Red, an anionic dye, was used as a model of anionic compound to be trapped by modified materials.

## 2. Materials and Methods

### 2.1. Chemicals

$Mg(NO_3)_2 \cdot 6H_2O$ (99%) was obtained from Sigma Aldrich (India). NaOH (97%), $Ru(NH_3)_6Cl_3$ (98%), 1,1'-ferrocene dimethanol (96%), $K_3Fe(CN)_6$ (99%), Congo Red (≥85%) and tetradecyldimethyl(3-trimethoxysilylpropyl)ammonium chloride came from Sigma Aldrich (St Louis, USA). $Al(NO_3)_3 \cdot 6H_2O$ (98–102%) and concentrated HCl (37%) were purchased from Carlo Erba (Val de Reuil, France), and $Na_4SiO_4$ provided by AlfaAesar (Karlsruhe, Germany). Deionized water (18.2 MΩ) was used for the preparation of solutions and clay mineral suspensions.

### 2.2. Synthesis and functionalization of saponite

The synthesis of saponite was performed following the protocol described in Meyer et al. [26]. Briefly, the precursor with Al/Si/Mg molar ratio of 0.5/3.5/3 was prepared by mixing 0.2 M solution of $Mg(NO_3)_2$ with 0.2 M solution of $Al(NO_3)_3$, followed by the addition of 0.2 M solution of $Na_4SiO_4$. The obtained suspension was dried at 200°C, then calcined at 450°C during 1 hour. The obtained powder was treated hydrothermally at 200°C for 5 days in 70 mL of NaOH solution at pH=12. The synthesis product was recovered and washed three times with deionized water by centrifugation at 8000 rpm (9946×$g$) for 10 min, dried at 60°C and grinded in mortar (sample labeled "Sap").

Prior to the functionalization, saponite was treated with 0.1 M HCl for 24 hours with solid/solution ratio 20 $g \cdot L^{-1}$. The solid was recovered and washed three times with deionized water by centrifugation at 8000 rpm (9946×$g$) for 10 min, dried at 60°C and grinded in mortar (sample labeled "Sap-H").

Sap and Sap-H were functionalized with tetradecyldimethyl(3-trimethoxysilylpropyl)ammonium chloride (abbreviated further as alkoxysilane) putting 0.250 g of the solid in contact with 15 mL of ethanol followed by the addition of 150 µL of

alkoxysilane and leaving the suspension under stirring at 60°C for 2 hours. Thus, the introduced quantity of alkoxysilane was $1.20 \cdot 10^{-3}$ mol per gram of saponite, corresponding to the cation exchange capacity of solid. The product was recovered and washed three times with ethanol by centrifugation at 8000 rpm (9946×*g*) for 10 min, then dried at 120°C for 12 hours (samples labeled "Sap-F" and "Sap-H-F" when the precursor was Sap or Sap-H, respectively).

### 2.3. Characterization of materials

To obtain the information about the chemical composition and structure of materials, they were characterized by X-ray diffraction (XRD), scanning electron microscopy (SEM) coupled with energy dispersive X-ray spectroscopy (EDX), Fourier-transform infra-red spectroscopy (FTIR), nuclear magnetic resonance spectroscopy (NMR) and thermogravimetric analysis (TGA).

The information about sample structure was obtained from powder XRD. Samples were prepared by mortar-and-pestle grinding, and back-loaded in the sample holder. The measurements were performed with X'Pert Pro instrument from Malvern PANalytical (United Kingdom) equipped with a PIXcel real-time multiple strip detector (active length=3.347° 2θ) over the 2°–70° 2θ range using CuKα radiation (λ=1.542 Å). The diffractograms were acquired with step size of 0.013°2θ and a time per step of 1.2 s. The fixed divergence slit, the anti-scatter slit, and the two Soller slits were 0.0625, 0.125, and 2.3°, respectively. The relative humidity was not controlled, but monitored to be constant during the XRD experiments.

The texture and chemical composition of samples were determined using a JSM-7900F scanning electron microscope from JEOL (Tokyo, Japan) equipped with an energy dispersive X-ray spectrometer composed of two XFlash 6-30 X-ray detectors from Bruker (Billerica, USA). In order to provide sufficient resolution to observe the fine structure of saponite, SEM images were acquired using in-lens electron detector, 2 kV specimen bias voltage and 2 kV landing voltage. Chemical compositions of studied samples were obtained by quantitative analyses at 15 kV using PhiRhoZ method and a reference saponite with known composition as standard. For the chemical analysis, samples were prepared by pressing them in pellets and the average value of 9 measurements was considered in order to approach as much as possible the bulk composition of the sample.

The bonding of elements in the samples was studied by FTIR. Samples were prepared by mixing an aliquot with potassium bromide at a mass ratio of 1:100 followed by grinding with mortar-and-pestle and pressing the powder into a 13 mm pellet at 4 bar for 2 min. The pellets were dried at 150°C overnight prior to analysis. The measurements were conducted with an Equinox IFS 55 instrument equipped with a DTGS detector from Bruker (Karlsruhe, Germany). The reported spectra are the average of 32 measurements with a resolution of 4 $cm^{-1}$. The software OPUS was used to record the spectra and to subtract the reference with $CO_2$ and $H_2O$ contributions.

The environment around different type of Si atoms in the material structure was studied by $^{29}Si$ NMR spectroscopy. $^{1}H$ decoupled $^{29}Si$ MAS NMR and $^{1}H$–$^{29}Si$ Cross Polarization Magic Angle Spinning (CPMAS) NMR spectra were recorded at room temperature on a Bruker Avance NEO 300WB spectrometer ($B_0$=9.4 T) operating at $B_0$ = 7.1 T giving Larmor frequencies of 59.61 MHz for $^{29}Si$ and 300.08 MHz for $^{1}H$. Samples were packed in a 7 mm diameter cylindrical zirconia rotor fitted with Kel-f end caps and spun at a spinning frequency of 4 kHz. $^{1}H$–$^{29}Si$ CPMAS NMR experiments were performed with a proton π/2-pulse duration of 5.2 μs, a contact time of 4 ms, and a recycle delay of 1 s. $^{1}H$ spin lattice relaxation time ($T_1$) was measured with the inversion-recovery pulse sequence. The number of scans varied from 2000 to 7800 depending on the particular sample. $^{1}H$ decoupled $^{29}Si$ MAS NMR spectra were recorded with a silicon π/6-pulse duration of 1.75 μs, a recycle delay of 80 s and a $^{1}H$ high-power decoupling of 67 kHz. $^{29}Si$ chemical shifts are reported relative to external Tetramethylsilane (TMS).

The amount of grafted alkoxysilane was estimated using TGA. In typical analysis, 15 to 20 mg of sample were heated from 30°C to 1000°C at a ramp of 10°C·$min^{-1}$ in air flow of 100 mL·$min^{-1}$ using a Mettler – Toledo TGA/DSC1 LF1100 device (Switzerland). The grafted amount $g_{sil}$ (mmol·$g^{-1}$) was obtained from Eq.1.

$$g_{sil} = \frac{m_{sil}}{m.M_{sil}} 1000 \qquad \text{(eq.1)}$$

where $M_{sil}$ represent the molecular mass of the alkoxysilane (440.18 g·$mol^{-1}$), $m_{sil}$ (g) the mass of alkoxysilane determined in a given mass m (g) of the organoclay.

The mass of alkoxysilane $m_{sil}$ was determined using Eq.2.

$$m_{sil} = \frac{m_{200}.m_{sap(1000)}}{m_{sap(200)}} - m_{1000} \quad \text{(eq.2)}$$

where $m_{200}$ (g) and $m_{Sap(200)}$ (g) correspond to the mass of modified material and saponite, respectively, after the loss of physisorbed water (at 200°C), $m_{1000}$ (g) and $m_{Sap(1000)}$ (g) the mass of modified material and saponite, respectively, at the end of thermogravimetric analysis (complete dehydroxylation at 1000°C).

The grafting yield (%) was estimated considering the grafted amount with respect to the initially introduced amount of alkoxysilane of $3.1 \cdot 10^{-4}$ mol.

### 2.4. Electrochemical experiments

The glassy carbon electrode (GC) with a diameter of 3 mm was polished on a polishing cloth using abrasive alumina slurry (0.5 µm particles diameter) and thoroughly rinsed with deionized water. An aqueous suspension of pristine or modified saponite (2 $g \cdot L^{-1}$) was prepared by ultrasound dispersion of 4 mg of the material in 2 mL of deionized water. 10 µL of this suspension was deposited at the surface of GC and dried at room temperature for 2 h. During electrochemical characterization experiments, the working electrode, reference electrode (Ag/AgCl) and counter electrode (platinum wire) immersed in the electrolytic solution (KCl 0.1 M) were connected to a PGSTAT12 Autolab (Metrohm) potentiostat controlled by the General Purpose Electrochemical System (GPES) software. This setup was used to record multi cyclic volatommograms in electrolytic solution containing the different electrochemical probes (cationic ($Ru(NH_3)_6^{3+}$), anionic ($Fe(CN)_6^{3-}$) and neutral (1,1'-ferrocene dimethanol)). Electrochemical impedance spectroscopy data were collected in $Fe(CN)_6^{3-/4-}$ equimolar mixture (0.1 mM) and nyquist plots used to determine the charge transfer resistance.

### 2.5. Congo Red adsorption

In typical Congo Red (CR) adsorption experiment, the clay mineral (10 mg or 5 mg) was introduced in a vial containing 5 mL of CR solution. The mixture was stirred for 5 h and the UV-Vis spectra of the supernatant (collected by centrifugation) was recorded on a GENESYS 10S UV-vis spectrophotometer from Thermo Scientific. Residual CR concentration was determined using the absorbance at 498 nm and the corresponding calibration curve plotted using CR standard solutions. During adsorption experiments, the pH of the solution was not

adjusted and was in the range 5.3 – 5.5. At such pH, CR was in its anionic form in solution during the experiments, attested by the characteristic red color of the mixture.

# 3. Results and discussion

## 3.1. Structure and chemical composition of pristine and modified saponite

X-ray diffractograms of saponite (Figure 1) showed the characteristic peaks of this clay mineral corresponding to (00$\ell$), (020), (110), (200), (311), (060) and (332) crystallographic planes and confirming the successful synthesis of the material [31]. The $d_{001}$-value, characteristic of the layer-to-layer stacking of clay minerals, was 12.6 Å and indicated the presence of hydrated sodium cations in the interlayer space. The acid treatment did not significantly alter the structure of saponite as the peak positions of (*hk*$\ell$) planes remained unchanged (Figure 1). Only, the position and shape of diffraction peaks corresponding to (00$\ell$) planes were slightly impacted. Indeed, after the acid treatment, the peak corresponding to (001) plane decreased in intensity and shifted from 12.6 to 13.3 Å. The acid treatment certainly induced some exchange of the interlayer cations and thus modified the layer-to-layer distance [32].

After the functionalization, the X-ray diffractograms of Sap and Sap-F were almost perfectly superimposable. Only the (001) reflection of Sap broadened slightly, indicating minor increase of the heterogeneity of the sample due to the presence of layers with different layer-to-layer distances (Figure 1). For the acid-treated sample the functionalization lead to an increase of average layer-to-layer distance (the $d_{001}$-value changed from 13.3 to 14.9 Å) and significant change of the peak shape, suggesting the intercalation of the alkoxysilane.

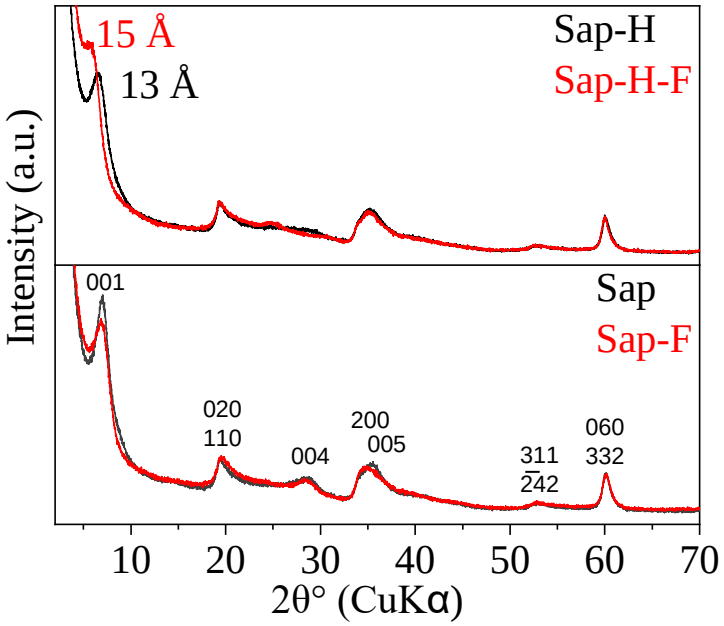


**Figure 1.** X-ray diffractograms of saponite and functionalized saponite in bottom panel; acid-treated saponite and acid-treated functionalized saponite in top panel.

The morphology of saponite and acid treated saponite particles was visualized by recording SEM micrographs (Figure 2). The "Sap" images showed randomly dispersed particles with sharp edges. After the acid treatment (sample "Sap-H"), the edges of the particles became noticeably less sharp. It was also difficult to observe individual particles. This clearly showed that the acid treatment modified the external surface of saponite particles. Following the modification with the alkoxysilane (Sap-F and Sap-H-F in Figure 2), even Sap particles became less well-defined, due to the presence of the organic matter adsorbed onto external surfaces.

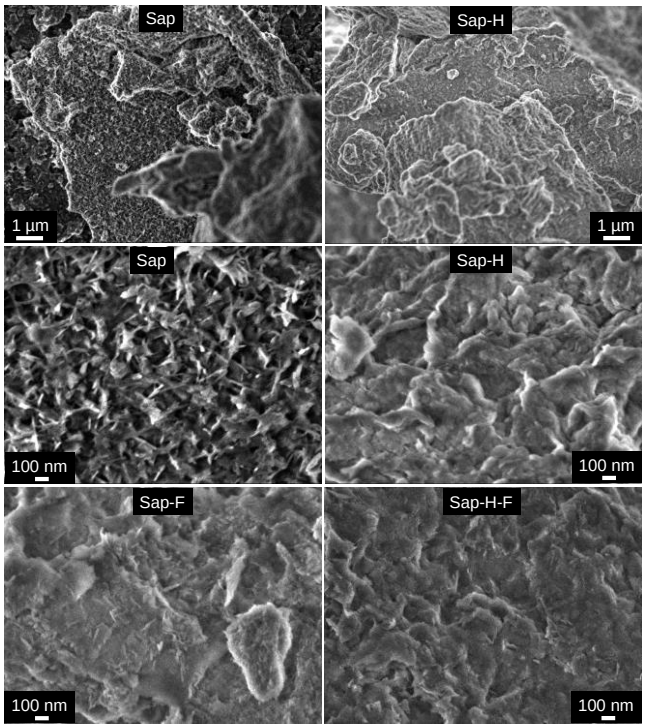


**Figure 2**. SEM images of saponite and acid-treated saponite, before (Sap and Sap-H, respectively) and after modification with the alkoxysilane (Sap-F and Sap-H-F, respectively).

Chemical compositions of saponite and acid treated saponite were determined by EDX analysis (Table 1). The chemical composition of synthesized saponite agreed well with the expected formula of $^{INT}Na_{0.50}{}^{TET}[Si_{3.50}Al_{0.50}]^{OCT}[Mg_3]O_{10}(OH)_2$, with some extra Mg (0.21 mol/$O_{10}(OH)_2$) and Al (0.03 mol/$O_{10}(OH)_2$) in the interlayer or on the external surface. After the acid treatment, a 50% decrease of sodium was observed, suggesting its replacement by $H^+$, in agreement with XRD results. The remaining structure was left intact with slight increase of Mg and Al content expected to be dissolved and re-adsorbed on clay mineral surface [33]. Initially, the acid treatment was chosen to increase the amount of silanol groups on clay mineral surface expected to favor the grafting of alkoxysilane, however as shown by the experimental results, other two phenomena are co-occurring: $H^+$-for-$Na^+$ exchange and partial dissolution of clay mineral surface.

**Table 1**. Chemical composition of synthesized ("Sap") and acid-treated saponite ("Sap-H").

| Molar % | O | Na | Mg | Al | Si |
|---|---|---|---|---|---|
| Sap | 58.5 | 2.9 | 17.1 | 2.8 | 18.6 |
| Sap-H | 59.2 | 1.5 | 17.6 | 3.1 | 18.6 |

The FTIR spectrum of Sap (Figure 3) presented characteristic bands of the clay mineral (MgO-H stretching vibration at 3684 $cm^{-1}$, Si-O at 1082 $cm^{-1}$ and 997 $cm^{-1}$, and Al-O-Si at 720 $cm^{-1}$ and 520 $cm^{-1}$) and confirmed once again the successful synthesis of saponite. Sap also presented high amount of water molecules (broad stretching vibration band of hydrogen-bonded water molecules at 3450 $cm^{-1}$ and bending vibration at 1640 $cm^{-1}$) adsorbed both on the external and the interlayer surfaces. Acid treatment (Sap-H) showed insignificant modification of the FTIR spectrum and suggested minor changes of the structural chemical bonds in Sap sample, in agreement with XRD and EDX results.

New bands assigned to aliphatic C-H stretching vibrations (2959 $cm^{-1}$, 2928 $cm^{-1}$ and 2854 $cm^{-1}$) and bending vibrations (1472 $cm^{-1}$) appeared on the spectra of Sap-F and Sap-H-F after reacting the material with the alkoxysilane [34]. These intense bands indicated that considerable amount of alkoxysilane was effectively present on saponite surface. The complete list of identified bands and the corresponding bond vibrations is presented in Supporting Information Table S01.

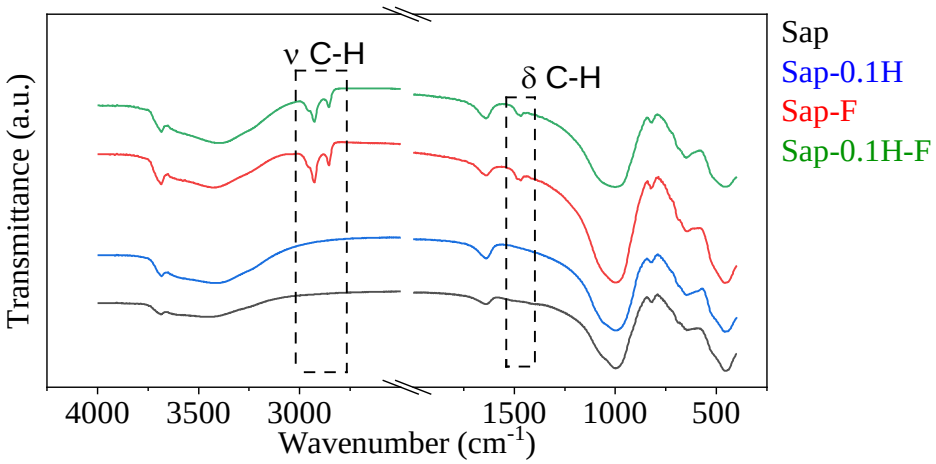


**Figure 3.** FTIR spectra of saponite, acid-treated saponite, functionalized saponite and acid-treated functionalized saponite.

$^{29}Si$ NMR spectroscopy was used to elucidate structural modification of saponite following acid treatment and alkoxysilane grafting. The different silicon nuclei are denoted $Q^n$ and $T^n$. Q and T correspond to tetra- and tri- functional units (four and three oxygen atoms surrounding the silicon atom, respectively) and *n* is the number of neighbor silicon atoms in the second

coordination shell. The $^{29}$Si NMR spectrum of saponite and acid treated sample (Figure 4) showed the well-known two sharp and intense peaks at -94 ppm and -89 ppm, and a shoulder at -85 ppm [35]. The peak at -94 ppm corresponds to trioxo coordinated framework silicon having no neighboring Al substitution ($Q^3$(0Al)). The peak at -89 ppm also corresponds to trioxo coordinated silicon, but with one neighboring Al substitution ($Q^3$(1Al)). Lastly, the shoulder at -85 ppm is attributed to silanol groups at the edge surface ($Q^2$(OH)). These results confirmed the poor structure alteration of the clay mineral following the acid treatment. The modification with alkoxysilane resulted in the presence of additional peaks ($T^1$ at –48 ppm, $T^2$ at –57 ppm and $T^3$ at –65 ppm) assigned to the silicon signal of the organic modifier [36]. The most intense $T^2$ peak indicated the formation of Si-O-Si bonds with neighbor grafted alkoxysilane on saponite surface. If the CPMAS spectra proved the grafting, and therefore the functionalization of the surface of saponites, they did not allow to estimate the quantity of grafted alkoxysilane. Consequently, the $^{29}$Si MAS spectra of each saponite were performed. Unfortunately, the low sensitivity of this technique combined with the low quantity of organic silicon made it impossible to observe the expected T-signals although a high number of accumulations were applied.

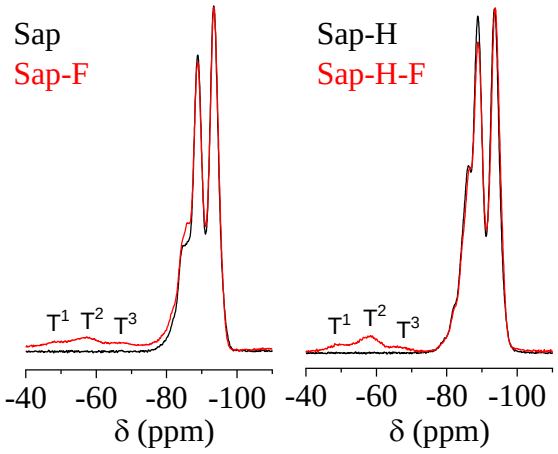


**Figure 4.** $^{29}$Si CPMAS NMR spectra of saponite and functionalized saponite on the left; acid-treated saponite and acid-treated functionalized saponite on the right.

To estimate the amount of alkoxysilane in the sample, thermogravimetric analysis was performed. The TGA of Sap and Sap-H (Figure 5) showed three thermal events frequently observed on saponite: the loss of abundant adsorbed water and dehydration (until 200°C) and dehydroxylation (400 – 800°C) [37]. After modification with alkoxysilane, additional mass loss in the range of 200 – 400°C was observed and assigned to the combustion of the organic

compound. The mass loss assigned to water molecules was reduced to the half, certainly due to the hydrophobic nature of the alkoxysilane. Meanwhile, their amount remained sufficiently important to consider that water molecules were still present. The amount of grafted alkoxysilane was determined accordingly to the Eq1 with the mass loss attributed to the alkoxysilane: 7.41 wt% and 7.94 wt% for Sap-F and Sap-H-F, respectively (Table 2). Very similar amount of alkoxysilane was thus grafted onto saponite, whether the material was acid treated or not corresponding to 0.15 and 0.16 mmol·g$^{-1}$ for Sap-F and Sap-H-F, respectively. The obtained result was of the same order of magnitude as previously reported for hectorite [12,13] and saponite [11,22], but significantly smaller than reported previously for montmorillonite [18,19]. Previous studies suggested three different interaction modes of alkoxysilane with clay mineral surface observed during thermal analysis : physically adsorbed, intercalated and grafted alkoxysilane [18]. A small difference between Sap-F and Sap-H-F noticeable on the derivative curve around 380°C suggested that some of the alkoxysilane could be intercalated between Sap-H-F layers.

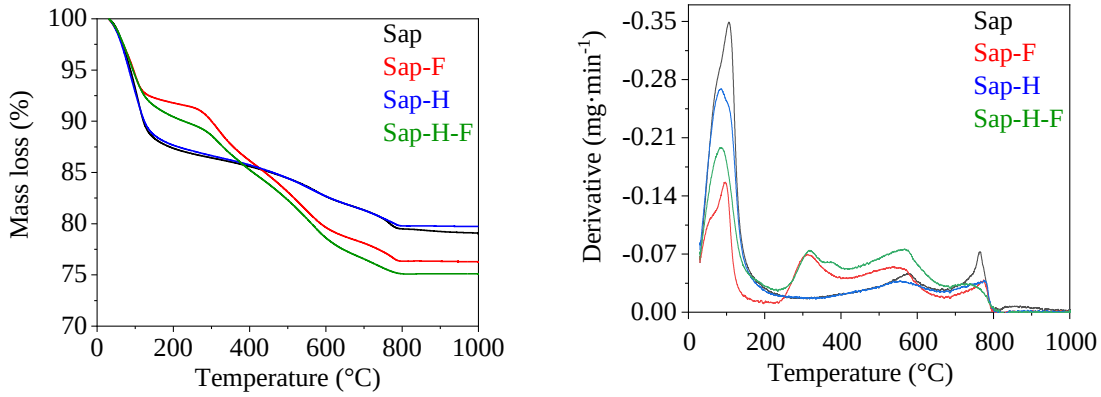


**Figure 5.** Thermogravimetric analysis (left) and its derivative (right) of saponite, acid-treated saponite, functionalized saponite and acid-treated functionalized saponite.

The results from different characterization techniques suggested that the acid treatment of saponite induced $H^+$-for-$Na^+$ cation exchange in the interlayer surface of clay mineral and favored a slight dissolution, which in turn induced $Mg^{2+}$-for-$Na^+$ cation exchange. On the other hand, the amount of grafted alkoxysilane on saponite and acid-treated saponite was similar. Thus, the acid treatment did not play a significant role for the surface modification of material regarding the surface silanol groups. Meanwhile, $H^+$-for-$Na^+$ cation exchange allowed a partial intercalation of alkoxysilane in the interlayer space of acid-treated saponite.

**Table 2.** Thermogravimetric analysis of functionalized saponite.

| | Mass loss (%) | Grafted amount ($mmol \cdot g^{-1}$) | Grafted yield (%) |
|---|---|---|---|
| Sap-F | 7.41 | 0.15 | 7.2 |
| Sap-H-F | 7.94 | 0.16 | 10.0 |

The different characterization methods did not reveal the presence of amorphous silica. Several washing cycles were conducted after the grafting reaction to remove any unreacted species. Thus, the possibility of auto-hydrolysis of the alkoxysilane forming amorphous silica was considered to be very unlikely.

### 3.2. Electrochemical characterization at glassy carbon electrode

Electrochemical methods are now considered as powerful tool for the characterization of clay minerals, since these methods can provide unique information on their surface properties. Being very sensitive, the electrochemical methods can highlight even minor changes resulting from the modification of clay minerals' surfaces [19,38,39]. A cationic ($Ru(NH_3)_6^{3+}$) and anionic ($Fe(CN)_6^{3-}$) electrochemical probes were used to identify the surface charge modifications resulting from the acid treatment and the grafting of the cationic alkoxysilane onto saponite.

80 consecutive cyclic voltammograms were recorded onto GC electrodes covered with thin film of unmodified or modified saponite, immersed in a $Ru(NH_3)_6^{3+}$ electrolytic solution. The shape of the recorded signals (Figure 6A and Figure S01) presented several similarities. A well-defined signal was recorded after the first complete forward and backward potential scan, due to the electrochemical reversible transformation of $Ru(NH_3)_6^{3+}$. Thereafter, the signal intensities gradually increased with the number of scans until equilibrium was achieved after about 50 cycles (Figure S01). This increase in signal intensity (not observed on GC) reflected the accumulation of $Ru(NH_3)_6^{3+}$ on saponite by ion exchange with the compensating cations ($Na^+$ and $H^+$). Similar behaviour is common with 2:1 clay minerals containing exchangeable cations in the interlayer space and was reported for smectite modified electrodes [19,39].

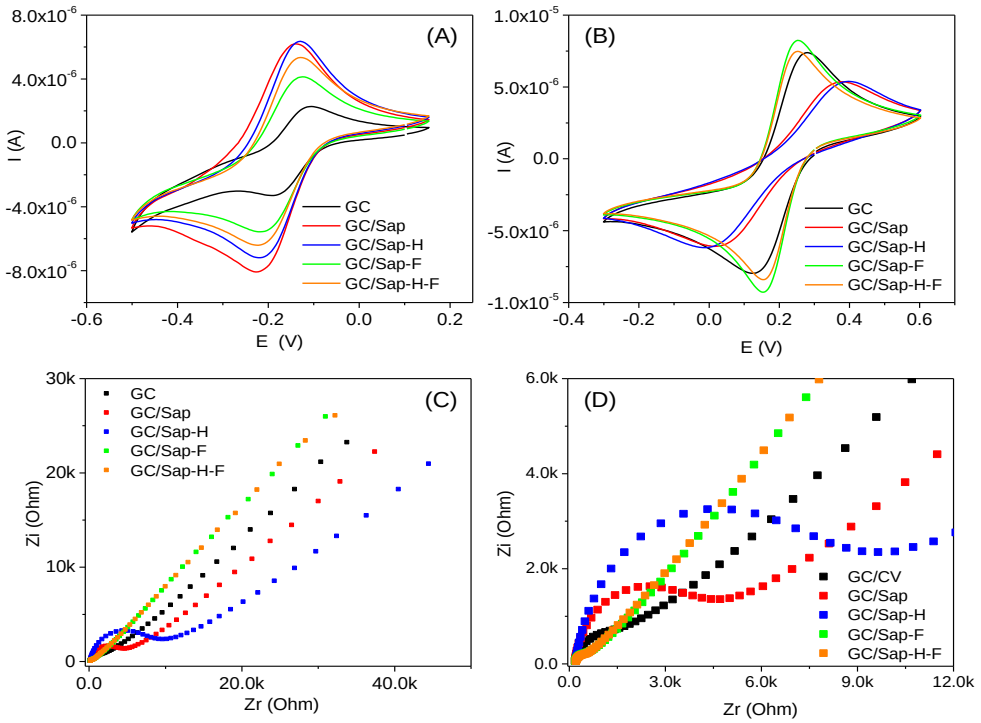


**Figure 6**. (A) Cyclic voltammograms at equilibrium recorded in KCl 0.1 M and $Ru(NH_3)_6^{3+}$ 0.2 mM on GC and clay mineral modified GC electrode. (B) Cyclic voltammograms at equilibrium recorded in KCl 0.1 M and $Fe(CN)_6^{3-}$ 1 mM on GC and clay mineral modified GC electrode. (C) Nyquist plots recorded in KCl 0.1 M and $Fe(CN)_6^{3-/4-}$ 1 mM on GC and clay mineral modified GC electrode. (D) Magnification of (C) to highlight the capacitive loops.

While such trend was predictable for Sap and Sap-H modified electrodes, it indicated that the alkoxysilane did not necessarily exchange completely the interlayer cations of the clay mineral during the grafting process. For an efficient signal comparison, only the signals at equilibrium were plotted in Figure 6A. Signals recorded on saponite-modified electrodes at equilibrium were at least two times more intense than those recorded on bare GC electrode. This indicated that the clay films increased the concentration of the analyte locally, confirming the suggested cation exchange mechanism. In addition, the presence of the alkoxysilane on saponite slightly decreased the signal intensity. This was probably the result of a partial replacement of exchangeable cations during the grafting reaction.

In the presence of the anionic probe $Fe(CN)_6^{3-}$, unlike bare GC electrode, the electrodes modified by Sap and Sap-H displayed a poorly defined and slow signal, marked by the increase of the separation of peak potentials (from 145 mV on GC to 355 mV on GC/Sap and

403 mV on GC/Sap-H) (Figure 6B). This reflected the barrier effect of the films that prevented the access of ferricyanide ions to the electrode surface. The saponite layers being negatively charged, they prevented the diffusion of anionic species through the film to reach the conductive glassy carbon electrode surface [39]. This barrier effect was however more marked on GC/Sap-H, certainly due to the acid treatment that increased the negative charge of the clay layers. On electrodes covered by films of alkoxysilane modified saponite (GC/Sap-F and GC/Sap-H-F), the signal became well defined, intense and faster (peak potentials separation of 98 mV) compared to the electrodes covered by the non-grafted saponite and even unmodified electrode. This demonstrated that the cationic alkoxysilane reduced the negative charge of the clay layers and resulted in a saponite organo-hybrid material displaying anionic exchanger properties. Despite this improvement of the reactivity of the anionic probe, accumulation effect was not observed on multicyclic voltammogramms (results not showed). This could be explained considering the grafting of the alkoxysilane mainly on the external surface of saponite.

In order to better highlight the differences between various materials concerning their interaction with anionic species, the electrochemical impedance spectroscopy in the presence of an equimolar mixture of $Fe(CN)_6^{3-/4-}$ was used for a further characterization of electrodes. The Nyquist diagrams obtained are presented in Figure 6C and D. These diagrams showed a similar trend: a capacitive loop at high frequencies (characterizing the charge transfer resulting from the electrochemical transformations involving the $Fe(CN)_6^{3-/4-}$ couple) and a straight line with a positive slope at low frequencies, associated to the diffusion of chemical species at the vicinity of the electrode surface. The diameter of the capacitive loops represented the charge transfer resistance, a parameter indicating the electron transfer kinetic between the electroactive species and the electrode surface. As expected, the electrodes modified by Sap and Sap-H exhibited the highest charge transfer resistances (9.67 kΩ and 4.31 kΩ, respectively). The greater charge transfer resistance value on GC/Sap-H confirmed the increase of the negative charge of saponite layers, following the acid treatment. The alkoxysilane modified saponite produced the lowest charge transfer resistance (524.72 Ω and 573.45 Ω for GC/Sap-H-F and GC/Sap-F, respectively) even compared to GC (1.55 kΩ).

A neutral organophilic probe (ferocene dimethanol) was also used for the characterization of the materials. The electrochemical signals recorded were fast and reversible as the ones recorded on bare glassy carbon electrode (Figure S02). The electrodes were thus expected to

exhibit similar interactions with respect to this compound. This result was certainly the consequence of the organophilic basal surfaces of saponite particles that controlled and favoured interactions between ferocene dimethanol and clay mineral particles.

Based on information obtained from characterization methods, the structures of pristine, acid pre-treated and silane functionnalized saponite are proposed in Figure 7.

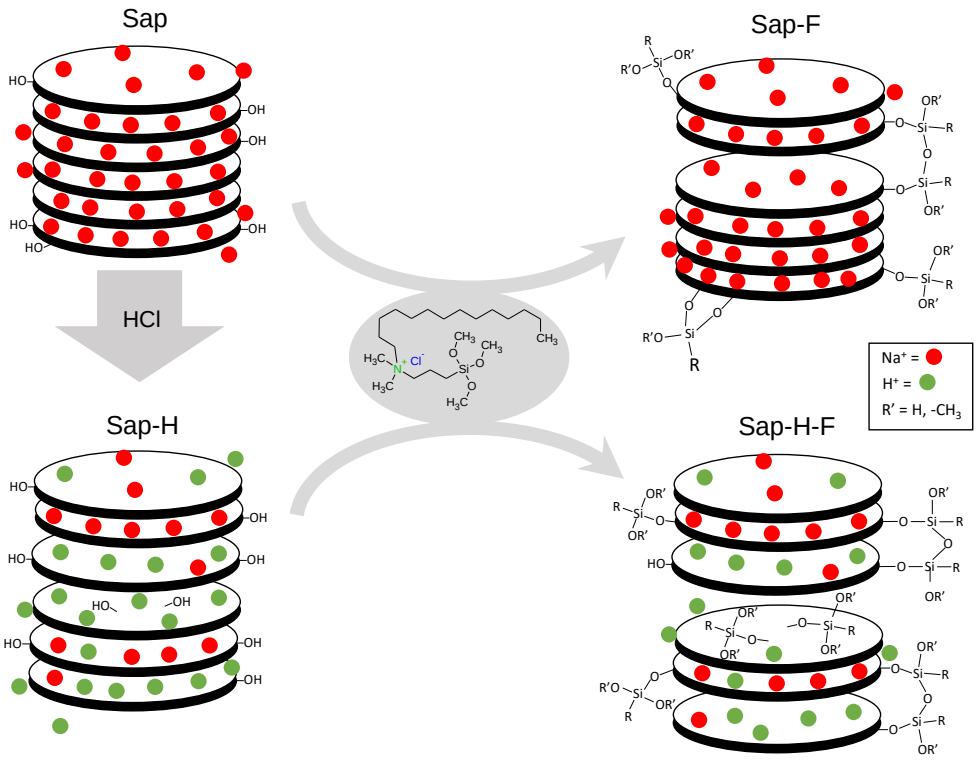


**Figure 7**. Schematic representation of change of saponite layer-to-layer stacking upon acid treatment and functionalization. Localization of functional groups and alkoxysilane grafting mode (monodentate, bidentate) are also highlighted.

Acid treatment increased the amount of –OH on the edge and interlayer surfaces and contributed to the increase of layer-to-layer distance due to $H^+$-for-$Na^+$ exchange. The functionalization after the acid pre-treatment resulted in alkoxysilane grafting with more significant layer-to-layer distance increase due to the intercalation of alkoxysilane in the interlayer surface of saponite and possibly due to the increased bidentate ($T^2$) grafting. The experimental results agree with literature reporting silylation of saponite particles [11,22]. The basal and interlayer surfaces of clay minerals are expected to contain very few surface ≡O-H groups, therefore the grafting onto these surfaces is very unlikely. It has to be noted that the presence of defects on basal and interlayer surfaces can generate some ≡O-H groups, but their

amount is expected to be negligible with respective to the presence of ≡O-H groups on the clay mineral edge surface.

### 3.3. Application for Congo Red adsorption

The ability of the modified saponite to accumulate anions was applied to the adsorption of Congo Red (CR), an anionic dye (selected as a model anionic organic compound). The structure of this dye is presented in the Supplementary Material (Scheme S01). Figure 8A depicts the UV-Vis spectra of 20 µM CR solutions before and after adsorption on pristine and modified saponite samples. The spectra recorded after adsorption on Sap and Sap-H showed intensities close to those of the solution before adsorption, indicating a poor adsorption of the dye molecules. This confirmed the poor affinity of these materials for anionic compounds revealed by the electrochemical characterization. This phenomenon was even more marked on Sap-H (the spectra were almost superimposed with those of the control experiment) because the acid treatment increased the anionic character of the saponite layers. The spectra recorded after adsorption on functionalized materials were practically superimposed to the baseline, indicating an almost complete adsorption of the dye. This once again confirmed the ability of the alkoxysilane modified saponite to adsorb anionic species.

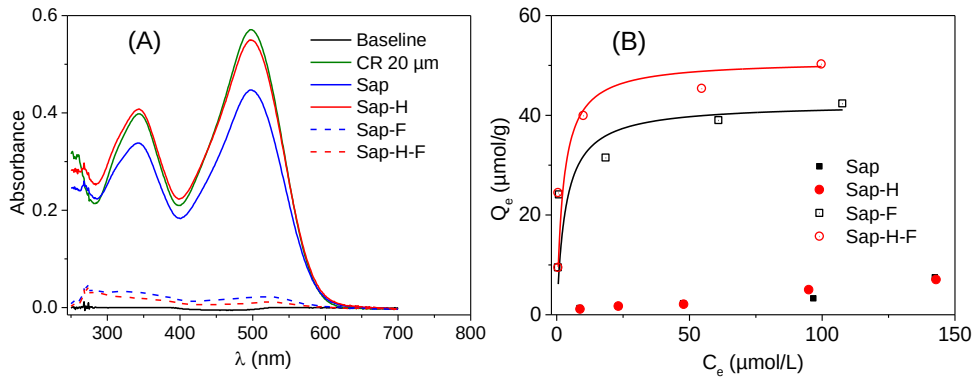


**Figure 8**. (A) UV-Vis spectra of 5 mL of 20 µM Congo Red solutions before and after 2 h of adsorption on pristine and modified saponite. (B) Adsorption isotherms of CR onto pristine and modified saponite.

For a more precise evaluation of the efficiency of different materials towards CR adsorption, the effect of dye concentration was systematically studied. Figure 8B shows the adsorption isotherms obtained for CR concentration range 10 µM to 150 µM. As expected, Sap and Sap-H showed almost no adsorption in the concentration range investigated. Sap-F and Sap-H-F

showed the typical trend of adsorption isotherms frequently obtained in solid/liquid adsorption: a fast increase of the adsorption capacity at low concentrations, reflecting the facile occupation of adsorption sites. This was followed by the formation of a plateau at high concentrations due to the saturation of adsorption sites. Despite these similar trends, Sap-H-F always exhibited the highest adsorption capacity in the whole concentration range investigated.

Two adsorption models (Langmuir and Freundlich) widely applied for adsorption experiments analysis were used for data fitting (See Table S02) [40]. The Langmuir model proved to be the most suitable model for the fitting of adsorption data on Sap-F and Sap-H-F ($R^2$ values> 0.99 against the Freundlich model $R^2$ values < 0.8). It was then used to evaluate the performance for CR adsorption. The maximum adsorption capacities obtained from the Langmuir model (42.7 µmol/g and 50.5 µmol/g for Sap-F and Sap-H-F, respectively) confirmed the best performance of Sap-H-F. The greater Langmuir constant on Sap-H-F (0.4 instead of 0.3 on Sap-F) also confirmed the preference of the dye for the functionalized acid pre-treated clay mineral.

## Conclusion

The characterization of functionalized clay mineral by different techniques indicated that grafting without acid pre-treatment resulted in the alkoxysilane oligomers attached to the saponite edge surface by one ($T^1$), two ($T^2$) or three ($T^3$) R-Si(-OR')$_3$ groups with only a very slight change of layer-to-layer distance. The increase of few layer-to-layer distances occurred due to bidendate ($T^2$) grafting. The acid treatment increased the grafted alkoxysilane amount only slightly and favoured the intercalation of alkoxysilane in the interlayer surface of clay mineral. The use of synthetic clay mineral revealed the complexity of grafting reactions, and further studies are needed to attempt to quantify this complexity. The electrochemical and adsorption tests confirmed that after the functionalization the cation exchange property of saponite was kept, and an anion exchange property was added in agreement with the conclusions drown from the characterization of material. Sap-H-F always exhibited the highest anion adsorption capacity. This collaborative study made it possible to verify and validate the conclusions obtained individually by two different approaches: characterization of material and test of its different properties. It allowed then to indisputably establish the link between the macroscopic properties and the structure of clay minerals at the nanometric scale.

## Acknowledgements

XRD, FTIR, SEM, NMR, and TGA analyses were performed on the technical platforms of IS2M. The authors are grateful to Laure Michelin, and Habiba Nouali for their contributions. ISP is acknowledged for the grant offered to the African Network of Electroanalytical Chemists (ANEC).

## References

[1] P. mondial de l'UNESCO pour l'évaluation des ressources en Eau, The United Nations world water development report 2021: valuing water, UNESCO, Paris, 2021. https://unesdoc.unesco.org/ark:/48223/pf0000375724.

[2] P. Djomgoue, M. Siewe, E. Djoufac, P. Kenfack, D. Njopwouo, Surface modification of Cameroonian magnetite rich clay with Eriochrome Black T. Application for adsorption of nickel in aqueous solution, Appl. Surf. Sci. 258 (2012) 7470–7479. https://doi.org/10.1016/j.apsusc.2012.04.065.

[3] J.W. Goodwin, R.S. Harbron, P.A. Reynolds, Functionalization of colloidal silica and silica surfaces via silylation reactions, Colloid Polym. Sci. 268 (1990) 766–777. https://doi.org/10.1007/BF01411109.

[4] T. Borrego, M. Andrade, M.L. Pinto, A. Rosa Silva, A.P. Carvalho, J. Rocha, C. Freire, J. Pires, Physicochemical characterization of silylated functionalized materials, J. Colloid Interface Sci. 344 (2010) 603–610. https://doi.org/10.1016/j.jcis.2010.01.026.

[5] N. Takahashi, K. Kuroda, Materials design of layered silicates through covalent modification of interlayer surfaces, J. Mater. Chem. 21 (2011) 14336. https://doi.org/10.1039/c1jm10460h.

[6] K. Chabrol, M. Gressier, N. Pebere, M.-J. Menu, F. Martin, J.-P. Bonino, C. Marichal, J. Brendle, Functionalization of synthetic talc-like phyllosilicates by alkoxyorganosilane grafting, J. Mater. Chem. 20 (2010) 9695. https://doi.org/10.1039/c0jm01276a.

[7] L. Su, Q. Tao, H. He, J. Zhu, P. Yuan, R. Zhu, Silylation of montmorillonite surfaces: Dependence on solvent nature, J. Colloid Interface Sci. 391 (2013) 16–20.

https://doi.org/10.1016/j.jcis.2012.08.077.

[8] H. He, Q. Tao, J. Zhu, P. Yuan, W. Shen, S. Yang, Silylation of clay mineral surfaces, Appl. Clay Sci. 71 (2013) 15–20. https://doi.org/10.1016/j.clay.2012.09.028.

[9] G.B.B. Varadwaj, K. Parida, V.O. Nyamori, Transforming inorganic layered montmorillonite into inorganic–organic hybrid materials for various applications: a brief overview, Inorg. Chem. Front. 3 (2016) 1100–1111. https://doi.org/10.1039/C6QI00179C.

[10] A. Di Gianni, E. Amerio, O. Monticelli, R. Bongiovanni, Preparation of polymer/clay mineral nanocomposites via dispersion of silylated montmorillonite in a UV curable epoxy matrix, Appl. Clay Sci. 42 (2008) 116–124. https://doi.org/10.1016/j.clay.2007.12.011.

[11] L.R. Avila, E.H. de Faria, K.J. Ciuffi, E.J. Nassar, P.S. Calefi, M.A. Vicente, R. Trujillano, New synthesis strategies for effective functionalization of kaolinite and saponite with silylating agents, J. Colloid Interface Sci. 341 (2010) 186–193. https://doi.org/10.1016/j.jcis.2009.08.041.

[12] Negrete, J.-M. Letoffe, J.-L. Putaux, L. David, E. Bourgeat-Lami, Aqueous Dispersions of Silane-Functionalized Laponite Clay Platelets. A First Step toward the Elaboration of Water-Based Polymer/Clay Nanocomposites, Langmuir. 20 (2004) 1564–1571. https://doi.org/10.1021/la0349267.

[13] L.M. Daniel, R.L. Frost, H.Y. Zhu, Edge-modification of laponite with dimethyl-octylmethoxysilane, J. Colloid Interface Sci. 321 (2008) 302–309. https://doi.org/10.1016/j.jcis.2008.01.032.

[14] M. Park, I.-K. Shim, E.-Y. Jung, J.-H. Choy, Modification of external surface of laponite by silane grafting, J. Phys. Chem. Solids. 65 (2004) 499–501. https://doi.org/10.1016/j.jpcs.2003.10.031.

[15] H. He, J. Duchet, J. Galy, J.-F. Gerard, Grafting of swelling clay materials with 3-aminopropyltriethoxysilane, J. Colloid Interface Sci. 288 (2005) 171–176. https://doi.org/10.1016/j.jcis.2005.02.092.

[16] W. Shen, H. He, J. Zhu, P. Yuan, R.L. Frost, Grafting of montmorillonite with different

functional silanes via two different reaction systems, J. Colloid Interface Sci. 313 (2007) 268–273. https://doi.org/10.1016/j.jcis.2007.04.029.

[17] M.E. Parolo, G.R. Pettinari, T.B. Musso, M.P. Sánchez-Izquierdo, L.G. Fernández, Characterization of organo-modified bentonite sorbents: The effect of modification conditions on adsorption performance, Appl. Surf. Sci. 320 (2014) 356–363. https://doi.org/10.1016/j.apsusc.2014.09.105.

[18] M. Asgari, U. Sundararaj, Silane functionalization of sodium montmorillonite nanoclay: The effect of dispersing media on intercalation and chemical grafting, Appl. Clay Sci. 153 (2018) 228–238. https://doi.org/10.1016/j.clay.2017.12.020.

[19] J.G.Y. Mbokana, G.K. Dedzo, E. Ngameni, Grafting of organophilic silane in the interlayer space of acid-treated smectite: Application to the direct electrochemical detection of glyphosate, Appl. Clay Sci. 188 (2020) 105513. https://doi.org/10.1016/j.clay.2020.105513.

[20] A.M. Shanmugharaj, K.Y. Rhee, S.H. Ryu, Influence of dispersing medium on grafting of aminopropyltriethoxysilane in swelling clay materials, J. Colloid Interface Sci. 298 (2006) 854–859. https://doi.org/10.1016/j.jcis.2005.12.049.

[21] F. Piscitelli, P. Posocco, R. Toth, M. Fermeglia, S. Pricl, G. Mensitieri, M. Lavorgna, Sodium montmorillonite silylation: Unexpected effect of the aminosilane chain length, J. Colloid Interface Sci. 351 (2010) 108–115. https://doi.org/10.1016/j.jcis.2010.07.059.

[22] Q. Tao, Y. Fang, T. Li, D. Zhang, M. Chen, S. Ji, H. He, S. Komarneni, H. Zhang, Y. Dong, Y.D. Noh, Silylation of saponite with 3-aminopropyltriethoxysilane, Appl. Clay Sci. 132–133 (2016) 133–139. https://doi.org/10.1016/j.clay.2016.05.026.

[23] M. Jaber, S. Komarneni, C.-H. Zhou, Synthesis of Clay Minerals, in: F. Bergaya, G. Lagaly, B. Theng (Eds.), Handb. Clay Sci., Elsevier, 2013: pp. 223–241. https://doi.org/10.1016/B978-0-08-098258-8.00009-2.

[24] J.T. Kloprogge, Synthesis of Smectite Clay Minerals: A Critical Review, Clays Clay Miner. 47 (1999) 529–554. https://doi.org/10.1346/CCMN.1999.0470501.

[25] D. Zhang, C.-H. Zhou, C.-X. Lin, D.-S. Tong, W.-H. Yu, Synthesis of clay minerals,

Appl. Clay Sci. 50 (2010) 1–11. https://doi.org/10.1016/j.clay.2010.06.019.

[26] S. Meyer, S. Bennici, C. Vaulot, S. Rigolet, L. Dzene, Influence of the precursor and the temperature of synthesis on the structure of saponite, Clays Clay Miner. 68 (2020) 544–552. https://doi.org/10.1007/s42860-020-00099-1.

[27] F. Carniato, G. Gatti, C. Bisio, An overview of the recent synthesis and functionalization methods of saponite clay, New J. Chem. 44 (2020) 9969–9980. https://doi.org/10.1039/D0NJ00253D.

[28] R. Trujillano, E. Rico, M.A. Vicente, M. Herrero, V. Rives, Microwave radiation and mechanical grinding as new ways for preparation of saponite-like materials, Appl. Clay Sci. 48 (2010) 32–38. https://doi.org/10.1016/j.clay.2009.11.018.

[29] L. Mercier, C. Detellier, Preparation, Characterization, and Applications as Heavy Metals Sorbents of Covalently Grafted Thiol Functionalities on the Interlamellar Surface of Montmorillonite, Environ. Sci. Technol. 29 (1995) 1318–1323. https://doi.org/10.1021/es00005a026.

[30] B. Paul, W.N. Martens, R.L. Frost, Organosilane grafted acid-activated beidellite clay for the removal of non-ionic alachlor and anionic imazaquin, Appl. Surf. Sci. 257 (2011) 5552–5558. https://doi.org/10.1016/j.apsusc.2011.01.034.

[31] H. Suquet, C. de la Calle, H. Pezerat, Swelling and structural organization of saponite, Clays Clay Miner. 23 (1975) 1–9. https://www.scopus.com/inward/record.uri?eid=2-s2.0-0016474834&partnerID=40&md5=6706ef471d37c37a6730dffce25fde16.

[32] L. Mareschal, J. Ranger, M.P. Turpault, Stoichiometry of a dissolution reaction of a trioctahedral vermiculite at pH 2.7, Geochim. Cosmochim. Acta. 73 (2009) 307–319. https://doi.org/10.1016/j.gca.2008.09.036.

[33] J.-C. Viennet, F. Hubert, E. Tertre, E. Ferrage, V. Robin, L. Dzene, C. Cochet, M.-P. Turpault, Effect of particle size on the experimental dissolution and auto-aluminization processes of K-vermiculite, Geochim. Cosmochim. Acta. 180 (2016) 164–176. https://doi.org/10.1016/j.gca.2016.02.005.

[34] G. Socrates, Infrared and Raman Characteristic Group Frequencies: Tables and Charts, 3rd ed., Wiley, 2004.

596 [35] J. Sanz, Chapter 12.7 Nuclear Magnetic Resonance Spectroscopy, in: F. Bergaya,
597 B.K.G. Theng, G. Lagaly (Eds.), Handb. Clay Sci., Elsevier, 2006: pp. 919–938.
598 https://doi.org/10.1016/S1572-4352(05)01033-0.

599 [36] M.C. Brochier Salon, P.A. Bayle, M. Abdelmouleh, S. Boufi, M.N. Belgacem, Kinetics
600 of hydrolysis and self condensation reactions of silanes by NMR spectroscopy,
601 Colloids Surfaces A Physicochem. Eng. Asp. 312 (2008) 83–91.
602 https://doi.org/10.1016/j.colsurfa.2007.06.028.

603 [37] S. Guggenheim, K.A.F. van Groos, Baseline Studies of the Clay Minerals Society
604 Source Clays: Thermal Analysis, Clays Clay Miner. 49 (2001) 433–443.

605 [38] G.K. Dedzo, S. Letaief, C. Detellier, Kaolinite-ionic liquid nanohybrid materials as
606 electrochemical sensors for size-selective detection of anions, J. Mater. Chem. 22
607 (2012) 20593–20601. https://doi.org/10.1039/c2jm34772e.

608 [39] I.K. Tonle, E. Ngameni, A. Walcarius, From clay- to organoclay-film modified
609 electrodes: Tuning charge selectivity in ion exchange voltammetry, Electrochim. Acta.
610 49 (2004) 3435–3443. https://doi.org/10.1016/j.electacta.2004.03.012.

611 [40] Y. Liu, Y.J. Liu, Biosorption isotherms, kinetics and thermodynamics, Sep. Purif.
612 Technol. 61 (2008) 229–242. https://doi.org/10.1016/j.seppur.2007.10.002.

613